Corrosion Behavior of Powder Metallurgy Y_2O_3 Dispersed Iron-and Nickel-Base Superalloys

M. Debata and G.S. Upadhyaya

(Submitted 17 October 2000; in revised form 30 April 2001)

The room-temperature corrosion behavior of iron-base MA956 and nickel-base MA754 superalloys was investigated in H_2SO_4 (0.1 to 5 N) and 0.6 N NaCl solutions using the potentiodynamic polarization technique. The study also includes x-ray diffraction and scanning electron microscopy (SEM) of the as-received and corroded surfaces. Both the alloys show good corrosion resistance to H_2SO_4. In the 0.6 N NaCl solution, the nickel-base superalloy MA754 was found to be more corrosion resistant as compared to the iron-base superalloy MA956.

Keywords mechanical alloying, pitting corrosion, potentiodynamic polarization

1. Introduction

Mechanical alloying (MA) provides a means for producing powder metallurgy (P/M) dispersion-strengthened alloys of widely varying compositions with a unique set of properties. One of the oxide dispersion-strengthened (ODS) P/M ferritic superalloys reported is MA 956, whose composition is based on conventional Kanthal. The advantages are its high melting point together with a low density and low thermal expansion and also its excellent oxidation and corrosion resistance. The major dispersoid is $3Y_2O_3 \cdot 5Al_2O_3$ together with some $Y_2O_3 \cdot Al_2O_3$. There is also some Ti(C,N), which has been found to be situated mainly on the grain boundaries with an average size of 200 nm of an angular shape. The Al_2O_3 particles are coarse and occasionally arranged in long stringers.

Nutting *et al.*,[1] using optical and transmission electron microscopy together with x-ray diffraction, studied grain structures, phase population, and the defect structures of MA 956 at several stages of the manufacturing process. The oxidation resistance of the ODS MA 956 is determined by the aluminum content, which is between 4 and 5 wt.%. Much more important than the integral aluminum content is the active aluminum portion dissolved in the matrix.

The superalloy MA 754 is basically an ODS Ni-Cr solid solution. The oxide dispersoid is yttrium aluminate formed by the reaction between added Y_2O_3, excess oxygen in the powder, and a trace of aluminum added to the getter oxygen. The mean particle size and volume fraction of the dispersoid in MA 754 are 15 nm and 1.3%, respectively.

In the present investigation, the corrosion behavior of Y_2O_3 dispersed iron-base MA956 grade and nickel-base MA 754 grade superalloys in H_2SO_4 media of different concentrations and 0.6 N NaCl has been studied.

M. Debata and **G.S. Upadhyaya,** Department of Materials and Metallurgical Engineering, Indian Institute of Technology, Kanpur 208 016, India. Contact e-mail: gsu@iitk.ac.in.

2. Experimental Procedure

The chemical compositions of the alloys and their relevant data are given in Table 1. These ODS alloys were produced by INCO (London, United Kingdom), using MA followed by conventional hot isostatic pressing and hot forging.[2] The cylindrical specimens of approximately 1.25 cm diameter were first ground flat on a grinding belt and then polished using a series of emery papers up to 1000 grit size. The final wet polishing was subsequently carried out on a polishing wheel using 0.3 μm size alumina powder suspension in distilled water. The samples were mounted in epoxy with electrical connections through the rear of the mounts.

Table 1 Chemical compositions and density data

Alloy	Density (g cm^{-3})	Nominal composition, wt.%						
Fe-base superalloy		C	Si	Cu	Mn	Cr	Ti	Al
(MA 956)	7.51	0.024	0.12	0.04	0.07	19.10	0.34	4.31
		Co	Ni	P	S	N	Y_2O_3	Fe
		0.02	0.24	0.005	0.004	0.028	0.48	bal
Ni-base superalloy		C	Fe	Cr	Ti	Al	S	P
(MA 754)	8.30	0.07	1.11	19.93	0.51	0.36	0.002	0.38
		Y_2O_3	Ni					
		0.59	bal					

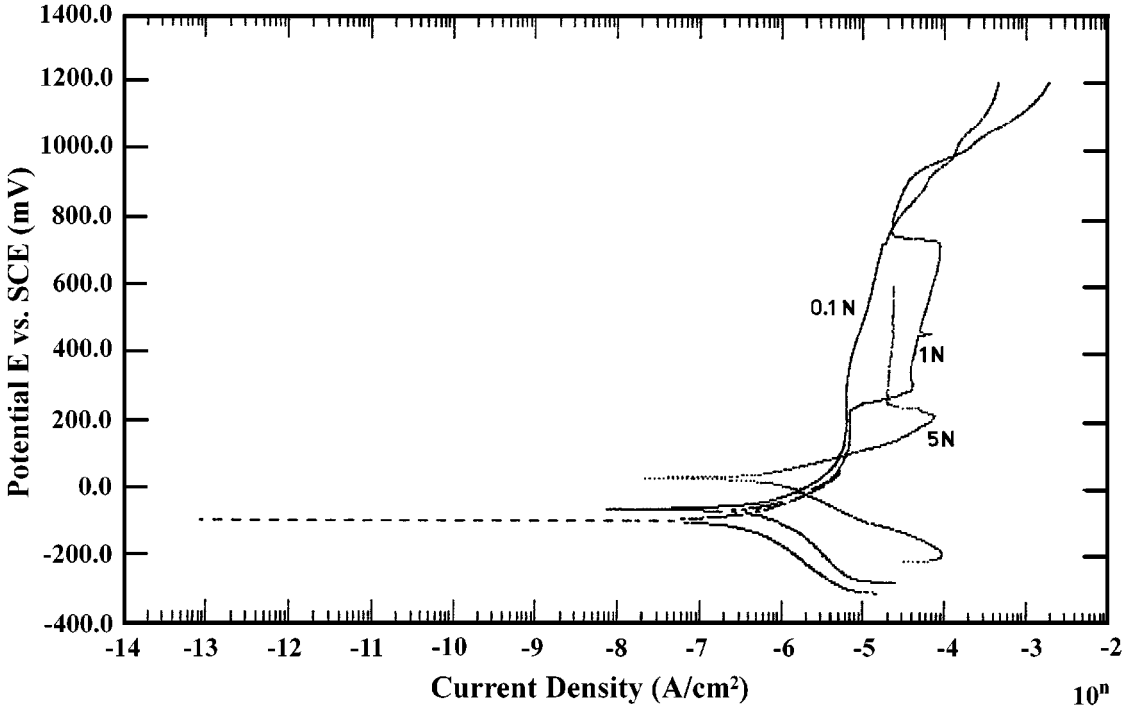

Fig. 1 Some typical anodic polarization curves of the Fe-base superalloy MA 956 in H_2SO_4 of various concentrations

Table 2 Anodic polarization characteristics of the superalloys in H_2SO_4 medium

Alloy	Concentration of H_2SO_4	E_{corr} (mV)	I_{corr} (μA/cm^2)	Corrosion rate	
				mpy	mmpy
Fe-base superalloy MA 956	0.1 N	−61.08	2.301	1.104	0.028
	1 N	−94.92	0.5972	0.286	0.0072
	2 N	57.25	21.84	7.186	0.182
	3 N	7.875	1.265	0.606	0.015
	5 N	30.80	0.757	0.363	0.0092
Ni-base superalloy MA 754	0.1 N	−85.68	2.420	1.069	0.027
	1 N	−119.7	1.698	0.749	0.019
	2 N	−46.45	1.946	0.858	0.021
	3 N	58.73	0.234	0.103	0.0026
	5 N	−221.3	1.341	0.591	0.015

Potentiodynamic scans for both alloys were taken with different concentrations of H_2SO_4 (0.1 to 5 N) and 0.6 N NaCl solutions. The polarization measurements were carried out using the EG& G Parc Model Versastat-II (Princeton, NJ) combined with the M352 programmer; the scanning rate was 1 mV/s. For testing, the samples were treated as the working electrodes and were connected in an electrical circuit, which allowed impression of an external voltage and measurement of corrosion current against the saturated calomel electrode. Graphite was used as the counterelectrode. The corrosion testing was carried out at room temperature.

The x-ray diffraction study of as-received and corroded surfaces was carried out with the help of an ISO Debyeflex-2002 x-ray diffractometer (Rich. Seiifert & Co., Ahrensburg, Germany) using Cu K_α radiation. The scanning micrographs of the corroded surfaces were taken using a JEOL 840 A scanning electron microscope (Japan Electron Optics Ltd., Tokyo).

3. Results

3.1. Corrosion in H_2SO_4 Media

Anodic Polarization Studies. Results of potentiodynamic polarization studies, carried out on both the superalloys in H_2SO_4 media, are presented in Fig. 1 and 2 and Table 2. With an increase in the concentration of H_2SO_4, the first increase in the E_{corr} value corresponds to 2 N, followed by a second increase at 5 N in the case of MA 956 and a decrease at 5 N in the case of MA 754. With an increase in the concentration of H_2SO_4, an increase in I_{corr} value corresponds to 2 N, followed by a further decrease in the case of MA 956, and a second increase at 5 N for MA 754.

Figure 1 also shows some typical anodic polarization curves of MA 956 in various H_2SO_4 concentrations. Curves for 0.1 N

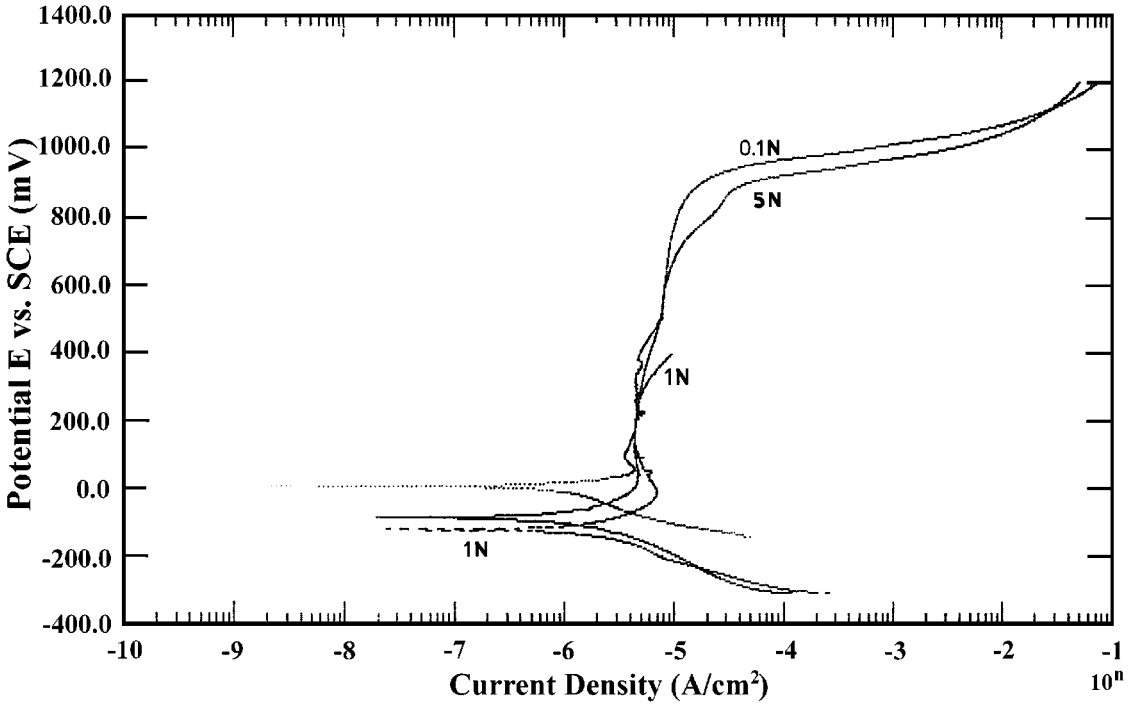

Fig. 2 Some typical anodic polarization curves of the Ni-base superalloy MA 754 in H_2SO_4 of various concentrations

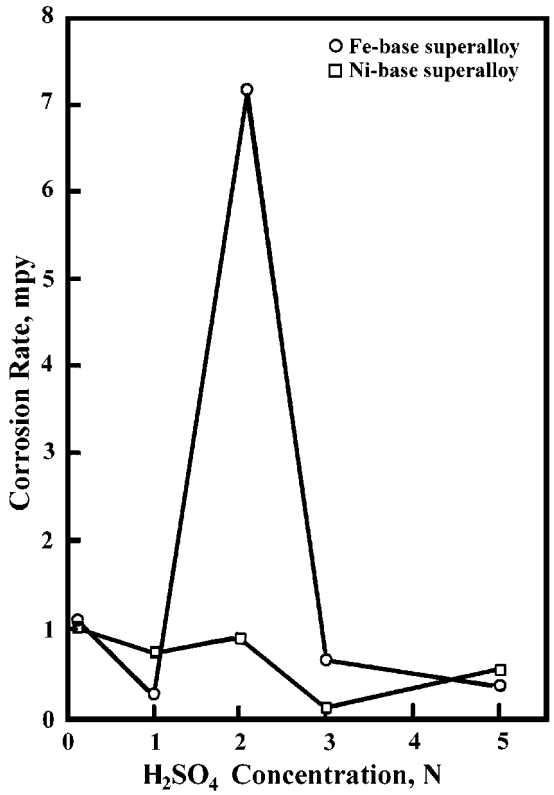

Fig. 3 Corrosion rate variation of Fe- and Ni-base superalloys with respect to H_2SO_4 concentration

show active, passive, and transpassive regions. The additional features of curves for 1 and 5 N are the prepassive region and secondary passive region, respectively. Figure 2 shows the anodic polarization curves for MA 754. Curves for 0.1 N show active, passive, and transpassive regions. The additional features of curves for 1 and 5 N is the prepassive region. For the sake of convenience, corrosion rates of both the alloys with respect to H_2SO_4 concentration are plotted in Fig. 3 from the data given in Table 2. A comparison of the two superalloys does not convey any clearcut relationship. The trend is similar to the variation of the I_{corr} value with the H_2SO_4 concentration.

Table 3 Anodic polarization characteristics of alloys in 0.6N NaCl solution

Alloy	E_{corr} (mV)	I_{corr} (μA/cm^2)	Corrosion rate	
			mpy	mmpy
Fe-base superalloy MA 956	−219.9	0.468	0.248	0.0058
Ni-base superalloy MA 754	−341.5	0.308	0.135	0.0034

Table 4 Lattice parameter (nm) variation of the matrix element of as-received and corroded alloys in different media

Alloy	As-received condition	Corroded condition	
		2N H_2SO_4	0.6N NaCl
Fe-base superalloy matrix	0.2890	0.2883	0.3171
Ni-base superalloy matrix	0.3558	0.3550	0.3558

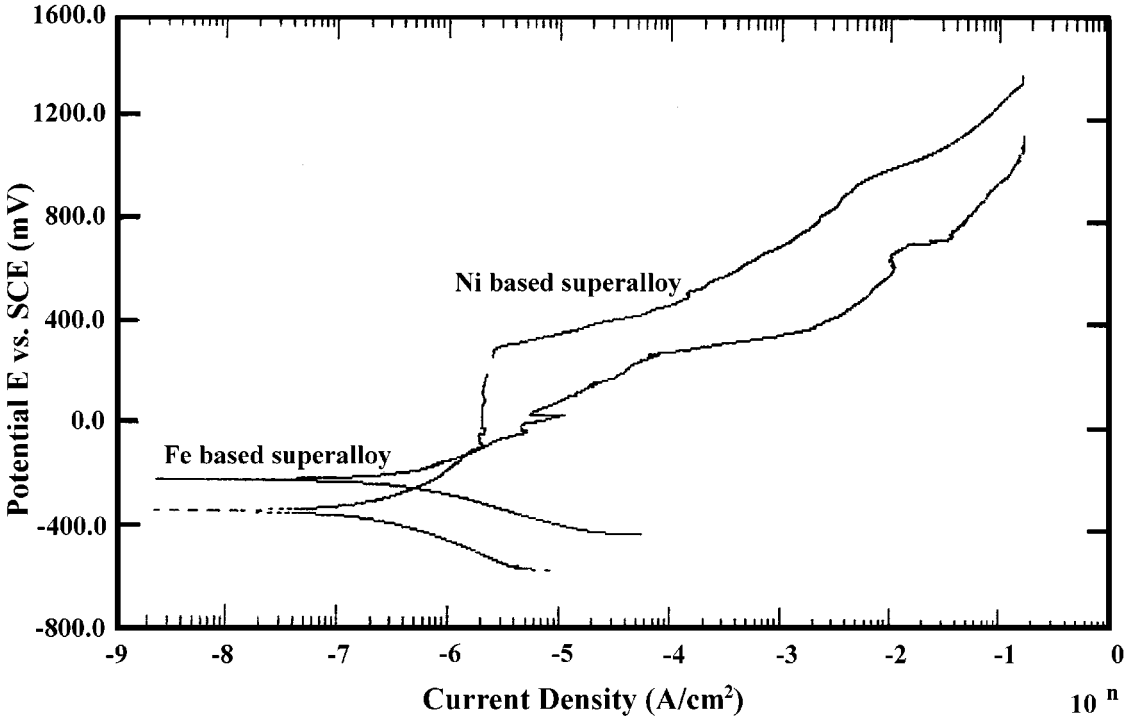

Fig. 4 Anodic polarization curves of Fe- and Ni- base superalloys in the 0.6 N NaCl solution

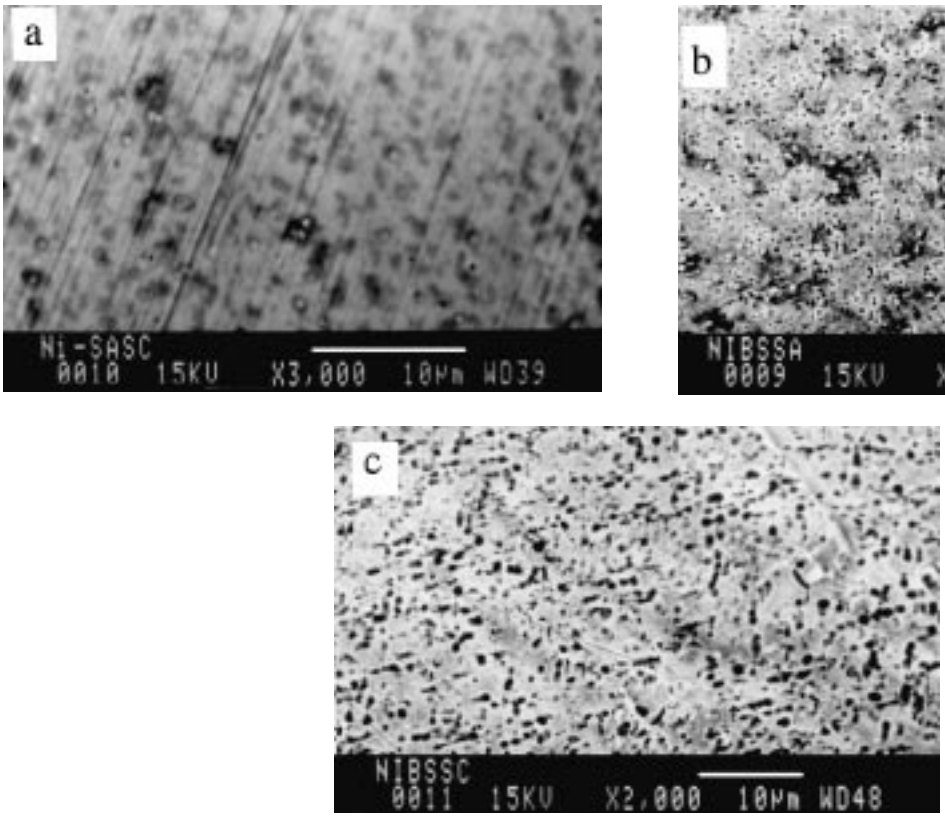

Fig. 5 SEM micrographs of the corroded surfaces of both alloys tested in 2 N H_2SO_4: (**a**) Fe-base superalloy MA956 and (**b**) through (**c**) Ni-base superalloy MA 754 at different magnifications

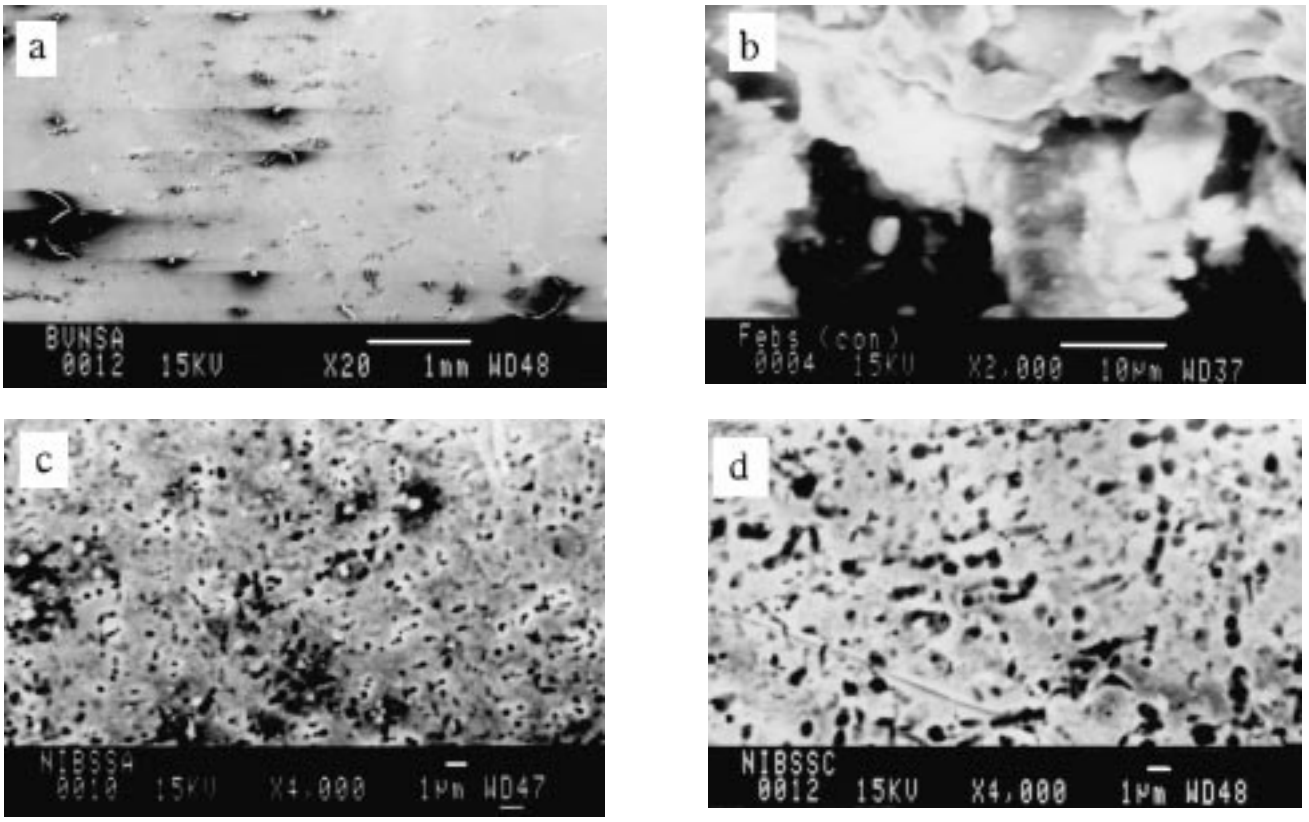

Fig. 6 SEM micrographs of the corroded surfaces of both alloys tested in the 0.6 N NaCl solution: (**a**) and (**b**) Fe-base superalloy at different magnifications and (**c**) and (**d**) Ni-base superalloy at different magnifications

X-ray Diffraction Studies. Due to the formation of relatively very thin oxide film at the surface of the alloys, no characteristic peaks for corresponding oxides were obtained. X-ray study was able to detect only the base elements. The lattice parameters for the base elements, *i.e.*, iron and nickel of as-received and corroded surfaces of the alloys, are given in Table 4.

Scanning Electron Microscopy Studies. The scanning electron microscopy (SEM) micrographs of the corroded surfaces corresponding to the 2 N H_2SO_4 solution for both alloys are shown in Fig. 5. The surface of Fe-base superalloy MA 956 is more affected compared to the Ni-base superalloy MA 754.

3.2. Corrosion in 0.6NNaCl

Anodic Polarization Studies. Results of potentiodynamic anodic polarization studies, carried out on these alloys in 0.6 N NaCl solution, are presented in Fig. 4 and Table 3. The curve for MA 754 shows clearly the active, passive, and transpassive regions. The corrosion rate for MA 956 is greater than that for MA 754. The former shows pitting corrosion to a greater extent.

X-ray Diffraction Studies. The lattice parameters for the base elements, *i.e.*, iron and nickel of as-received and corroded surfaces of the alloys, are given in Table 4.

SEM Studies. The SEM micrographs of the corroded surfaces of both alloys are shown in Fig. 6. In the case of Fe-base superalloy MA 956, corrosion pits on the surface were formed.

4. Discussion

4.1. Corrosion in H_2SO_4 Media

The anodic reactions involving iron and nickel in H_2SO_4 solution are

$$Fe \rightarrow Fe^{+2} + 2e \quad \text{(Eq 1)}$$

$$Ni \rightarrow Ni^{+2} + 2e \quad \text{(Eq 2)}$$

The cathodic reaction in both cases is the hydrogen ion reduction:

$$2H^{+} + 2e \rightarrow H_2 \quad \text{(Eq 3)}$$

Because the hydrogen ion is active, sulfate ion does not participate in the electrochemical reaction. The effect of increasing the concentration of H_2SO_4 on the corrosion rate does not follow a uniform pattern, first because of ionization effects in the aqueous solution and, second, because of changes that occur in the characteristics of the corrosion product film present on the surface of the metal. The literature[3] reports a linear behavior in the corrosion rate versus the H_2SO_4 concentration of iron within the concentration range of 25% (0 to 9.5 N). However, in the present case, no such linear curve

within that range was obtained. The plot obtained for MA 754 was also nonlinear.

Chromium improves the passivity of both alloys, which is quite evident from Fig. 1 and 2. Transpassive regions are clearly seen in the curves obtained for nickel-base superalloys. In the case of the iron-base superalloy, the presence of the prepassive state in the 5 N H_2SO_4 solution is supported by the results of Modi.[4]

4.2. Corrosion in NaCl Solution

Pitting corrosion usually occurs on those metals and alloys that show active to passive transition characteristics. In other words, metals that owe their corrosion resistance to the presence of thin and passive surface films may be susceptible to pitting attack when the surface film breaks down locally and does not reform. In a chloride environment, nickel is less susceptible for pitting than iron, *i.e.*, it has a higher pitting potential.[5] This feature is confirmed in Fig. 4. A corrosion pit is a unique type of anodic reaction, and the pits cathodically protect the rest of the alloy surface.

5. Conclusions

- In general, the superalloys investigated have good corrosion resistance in both H_2SO_4 and NaCl solutions.
- No regular trend in the behavior of the corrosion rate with respect to the concentration of H_2SO_4 is obtained, particularly for the iron-base superalloy MA 956.
- The nickel-base superalloy MA 754 is more corrosion resistant than the iron-base superalloy MA 956 in the 0.6 N NaCl solution.

References

1. J. Nutting, S. Ubhi, and T.A. Hughes: in *Frontiers of High Temperature Materials*, J.S. Benjamin, ed., Inco MAP, New York, NY, 1981, p. 33.
2. J.S. Benjamin: *Metall. Trans.*, 1970, vol. 1, p. 2943.
3. R. Ward: *Metals Handbook*, 8th ed., American Society for Metals, Metals Park, OH, 1975, vol. 10, p. 168.
4. O.P. Modi: Master's Thesis, Indian Institute of Technology, Kanpur, Aug. 1983.
5. J.B. Lumsden: *Conf. Proc. Int. Conf. Corrosion of Nickel-Base Alloys*, Cincinnati, OH, Oct. 23–25, 1984, ASM, Metals Park, OH, 1985, p. 183.